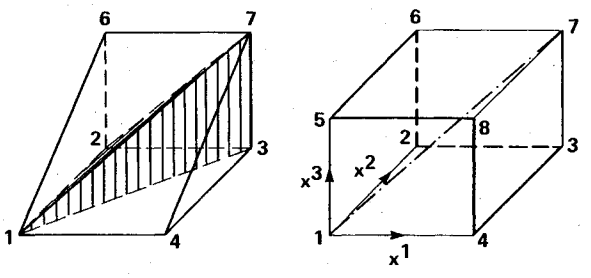

a) b)

Fig. 4 Suggested decomposition of the cell volume.

done in only two independent ways, as shown in Fig. 3. The decomposition of Fig. 3a is characterized by the fact that six of the eight corners are vertices of two surface diagonals, yielding the maximum number of 12 diagonal ends. The decomposition of Fig. 3b has two corners, each of which is the vertex of three diagonals, and six corners which are vertices of one diagonal. It turns out that the second decomposition yields a more convenient and simpler formula for the computation of the corresponding cell volume. For the computation of the volume consider, for example, the decomposition of the cell into two, as indicated in Fig. 4a. Each portion consists of three tetrahedra such that the total volume is given as

$$6\ \mathrm{Vol} = r_{71}\cdot[(r_{31}\times r_{21})+(r_{21}\times r_{61})+(r_{41}\times r_{31}) + (r_{81}\times r_{41})+(r_{51}\times r_{81})+(r_{61}\times r_{51})] \quad (2a)$$

$$= r_{71}\cdot[(r_{31}\times r_{24})+(r_{61}\times r_{52})+(r_{81}\times r_{45})] \quad (2b)$$

$$= 2r_{71}\cdot(S_{1485}+S_{1234}+S_{1562}) \quad (2c)$$

The expected six triple vector products reduce to three, having one single factor. They do not even require any volume calculations, since the surface vectors are available. Equation (2c) reflects the formula for calculating the volume of a pyramid: the complete cell consists of three topological pyramids with the three faces intersecting in r_1 as base surfaces and with r_7 determining the height with respect to each base. The volume for each pyramid is one-third of the corresponding height times the base surface, resulting in Eq. (2c) (see Fig. 4b). It is noted that for this kind of decomposition, four different volumes can be determined, depending on the choice of main diagonal of the general hexahedron.

Conclusions

In this Note we have shown how to compute efficiently the nonunique cell volume, based on a partitioning of cell surfaces with the same orientation on opposite faces. Because of its simplicity the new method is particularly suited to handle a time-dependent mesh. The computational effort involved is nominally reduced by at least 40%, compared with Ref. 1. In finite volume approaches where surface vectors are stored, the computational effort reduces further to the dot product of the chosen main cell diagonal with the sum of three surface vectors.

Acknowledgment

This research was partially supported by NASA Ames Research Center under Grant NCC 2-16.

References

[1] Rizzi, A. and Ericksson, L. E., "Transfinite Mesh Generation and Damped Euler Equation Algorithm for Transonic Flow Around Wing-Body Configurations," *AIAA Fifth Computational Fluid Dynamics Conference Proceedings*, June 1981, AIAA, New York, pp. 43-68.

[2] Coakley, T. J., "Numerical Method for Gas Dynamics Combining Characteristic and Conservation Concepts," AIAA Paper 81-1257, June 1981.

Unsteady Transonic Small Disturbance Approximation with Strong Shock Waves

G. David Kerlick* and David Nixon†
Nielsen Engineering & Research, Inc.
Mountain View, California
and
William F. Ballhaus Jr.‡
NASA Ames Research Center
Moffett Field, California

Introduction

THE most common methods of predicting steady flow aerodynamic characteristics at transonic speeds use either the transonic small disturbance (TSD) equation[1] or the full potential equation (FPE).[2] The more general Euler equations[3] are expensive to solve, although for flows with strong shock waves such solutions are essential. The FPE is derived on the assumption that the flow is isentropic and irrotational but it generally has a (numerically) exact treatment of the wing boundary conditions. The TSD equation is a further approximation to the full potential equation for small perturbations about freestream conditions. Thin wing boundary conditions are used in the solution procedure. There is some flexibility in deriving the TSD equation. This flexibility generally is utilized by a choice of a transonic scaling parameter. The basic assumptions of isentropy and irrotationality in both these theories are only valid when there are no shock waves in the flow, although a reasonable approximation to flows with shock waves is possible if the local Mach number just ahead of the shock is less than 1.3. If the flow has strong shock waves, however, then there is considerable disagreement between both TSD and FPE solutions and Euler equations solutions. Generally, the predicted shock location for the potential theories is much further aft than that for the Euler equations solutions. This is because the isentropic assumption is invalid in these flows. The causes of the error in the shock location in the steady TSD solutions for two-dimensional flow have been examined in Ref. 4 where a correction procedure has been derived that alters the basic equation within the formal accuracy bounds of the small disturbance approximation. A nonisentropic formulation for the full potential equation is given in Ref. 5. In the present paper, this procedure is extended to unsteady transonic flows, implemented in a modification to the low-frequency unsteady transonic small disturbance code LTRAN2,[6] and the results compared to solutions of the Euler equations.

Presented as Paper 82-0159 at the AIAA 20th Aerospace Sciences Meeting, Orlando, Fla., Jan. 11-14, 1982; submitted Jan. 22, 1982; revision received Oct. 13, 1982.

*Research Scientist. Member AIAA.
†Principal Scientist. Associate Fellow AIAA.
‡Director of Astronautics. Associate Fellow AIAA.

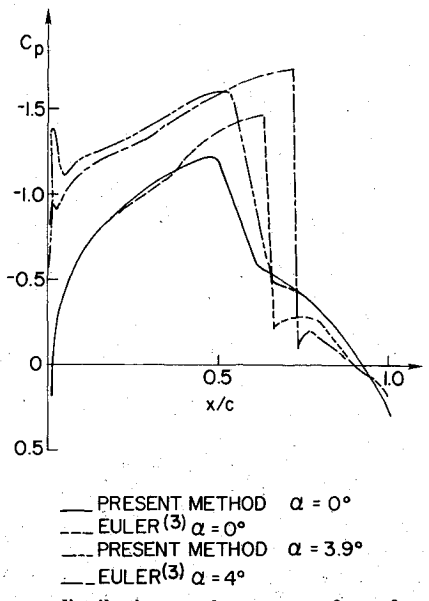

Fig. 1 Pressure distribution on the upper surface of an oscillating NACA 64A410 airfoil; $M_\infty = 0.72$, $\alpha = 2$ deg + 2 deg sin(ωt), $k = 0.2$.

Small Disturbance Equation—Basic Hypothesis

The low-frequency TSD equation for the perturbation velocity potential $\phi(x,y)$ at a freestream Mach number M_∞ may be written in the form[6]

$$(1-M_\infty^2)\phi_{xx}+\phi_{yy}=(\gamma+1)M_\infty^q\phi_x\phi_{xx}+(2M_\infty^2 c/U_\infty)\phi_{xt} \quad (1)$$

where γ is the ratio of specific heats, q the transonic scaling parameter, c the chord length, and U_∞ the freestream velocity. Powers higher than two of the perturbation velocity ϕ_x have been neglected in deriving Eq. (1). The pressure coefficient $C_p(x,y,t)$ is

$$C_p(x,y,t) = -2\phi_x(x,y,t) \quad (2)$$

Associated with Eq. (1) are the usual tangency and far field boundary conditions. The shock strength σ_T for a normal shock is

$$\sigma_T(t) = C_p^-(t) - C_p^+(t) = -2\left[C_p^+(t) - C_p^* + \frac{4M_\infty^2 c\dot{x}_s(t)}{(\gamma+1)M_\infty^q U_\infty}\right] \quad (3)$$

where C_p^+, C_p^- are the pressure coefficients just ahead of and behind the shock, $\dot{x}_s = (dx_s/dt)$ is the shock speed, and

$$C_p^* = \frac{-2(1-M_\infty^2)}{(\gamma+1)M_\infty^q} \quad (4)$$

For the low reduced frequencies $k = \omega c/U_\infty$ treated here, the term involving the shock speed is of the order $\mathcal{O}(\delta k)$, where $\delta \ll 1$ is the amplitude of the shock motion and, therefore, can be neglected. Thus,

$$\sigma_T \approx -2\{C_p^+(t) - C_p^*\} \quad (5)$$

When the same low-frequency assumption is made for the Euler equations, the quasisteady normal shock jump $\sigma_E(t)$ is given[7] by

$$\sigma_E(t) = \frac{2}{\gamma+1}[M_e^2(t)-1]\left(\frac{2}{\gamma M_\infty^2} + C_p^+(t)\right) \quad (6)$$

where the upstream shock Mach number M_e is given by

$$M_e^2(t) = \frac{1}{(\gamma-1)}\left\{[2+(\gamma-1)M_\infty^2]\Big/\left(\frac{\gamma}{2}M_\infty^2 C_p^+(t)+1\right)^{\frac{\gamma}{\gamma-1}} - 2\right\} \quad (7)$$

If the TSD (with $q = 2.0$) and Euler shock strengths are plotted against C_p^+ for $M_\infty = 0.755$ it can be seen[8] that as $|C_p^+|$ increases the discrepancy between σ_T and σ_E increases. It should be noted here that different transonic scalings not only give a different value of C_p^* but generally a different value of C_p^+. Thus, for different scalings the shock strength may vary considerably.

The present hypothesis, as in Ref. 4, is that the error in the shock location in both the steady and unsteady TSD solutions is due primarily to the error in the shock strength. Thus, if the TSD equation is altered, still within its formal accuracy bounds, such that the shock jump approximates the Euler equation shock jump, then the resulting equation should be a better compromise in representing the actual flow. By matching the shock jump the new equation implicitly introduces an additional mechanism (formally negligible) that cancels the entropy production and rotationality errors in a potential formulation.

Consider the more general form of Eq. (1)

$$f(\phi_x)\phi_{xx}+\phi_{yy}-2M_\infty^2(c/U_\infty)\phi_{xt}=0 \quad (8)$$

The normal shock jump relation is

$$F(\phi_x^+,\sigma) - 2M_\infty^2(c/U_\infty)\dot{x}_s = 0 \quad (9)$$

where ϕ_x^+ is the value of ϕ_x just ahead of the shock and σ is the shock strength. The function $F(\phi_x^+,\sigma)$ is given by

$$F(\phi_x^+,\sigma) = \frac{2}{\sigma}\int_{\phi_x^+-\frac{\sigma}{2}}^{\phi_x^+} f(\phi_x)\,d(\phi_x) \quad (10)$$

The problem is to pick a suitable form of $f(\phi_x)$. The ensuing conditions on $f(\phi_x)$ suggested the following conditions:

1) In general, $f(\phi_x)$ will be nonlinear in ϕ_x which leads to the possibility of multiple parabolic points, which occur whenever $f(\phi_x) = 0$. It is advisable that at least one of the roots of $f(\phi_x)$ be $\phi_{x_c^*}$ which is the parabolic point for a conventional (say Krupp) TSD solution. Thus,

$$f(\phi_{x_c}^*) = 0 \quad (11)$$

2) In order to avoid unrealistic multiple parabolic points in the domain of interest it is also desirable that $f(\phi_x)$ be a monotonically decreasing function in some range $\phi_{x_{\min}} \le \phi_x \le \phi_{x_{\max}}$. Thus,

$$\frac{df}{d(\phi_x)} < 0 \text{ for } \phi_{x_{\min}} \le \phi_x \le \phi_{x_{\max}} \quad (12)$$

3) The normal shock strength should be the same as the normal Euler shock strength. Neglecting the shock speed term in Eq. (8), as discussed in the previous section, gives

$$F(\phi_x^+,\sigma_E) = 0 \quad (13)$$

where σ_E is given by Eq. (6).

These three conditions, given in Eqs. (11), (12), and (13) will give the desired shock strength with no undesirable side effects. These conditions must be satisfied at each time step in order to get the correct shock jump. It is possible to reduce the amount of computational work required for an unsteady

example if a steady-state solution is first computed and the unsteady pressure distribution is related by a small perturbation to the steady-state result. Hence, if a modified small disturbance equation has been derived for the steady-state case it may be possible to use a simple analytic perturbation of the function $f(\phi_x)$ that will give good accuracy in the neighborhood of the steady-state result. The additional condition for this idea is given subsequently.

For the shock strength to be approximately correct over a range of values close to the steady-state value $\phi^+_{x_s}$, Eq. (13) can be expanded as a Taylor series to give

$$F(\phi^+_{x_s},\sigma_{E_s}) + \left[\left(\frac{\partial F}{\partial \phi^+_x}\right) + \frac{\partial F}{\partial \sigma_E}\frac{\mathrm{d}\sigma_E}{\mathrm{d}\phi^+_x}\right]_s (\phi^+_x - \phi^+_{x_s}) = 0 \quad (14)$$

where the subscript s denotes a value in the steady state.

Now, by definition

$$F(\phi^+_{x_s},\sigma_{E_s}) = 0 \quad (15)$$

and, hence, for Eq. (14) to be satisfied for a range of $(\phi^+_x - \phi^+_{x_s})$

$$\frac{\partial F}{\partial \phi^+_x} + \frac{\partial F}{\partial \sigma_E}\frac{\mathrm{d}\sigma_E}{\mathrm{d}\phi^+_{x_s}} = 0 \quad (16)$$

Thus, our method consists of satisfying Eqs. (11), (12), and (15) at each iterative step in the steady calculations and Eqs. (11), (12), and (16) at each time step in the unsteady calculation.

It is possible to derive functions $f(\phi_x)$ that satisfy all of the conditions given in the preceding section, but in a limited study, such as the present one, it is more convenient to satisfy only certain of these conditions explicitly and to test the resulting function with respect to the other conditions.

The most crucial conditions to satisfy are the shock strength conditions, Eqs. (15) and (16), since the object of the present exercise is to realize the correct shock strengths. Consequently, these conditions are satisfied explicitly. For simplicity in derivation, it is assumed that the modifications to the small disturbance equation will be sufficiently small that Eqs. (11) and (12), at least, will be approximately satisfied.

The form of $f(\phi_x)$ chosen is

$$f(\phi_x) = 1 - M^2_\infty + (\gamma+1)M^2_\infty(\phi^+_x/\phi^+_{x_s})^\alpha \phi_x + \epsilon\phi^2_x \quad (17)$$

Since powers of ϕ_x greater than two are neglected in the derivation of the small disturbance equation the term $\epsilon\phi^2_x\phi_{xx}$ is formally negligible. The exponent α is set equal to 1 during the steady iteration ($\phi^+_x = \phi^+_{x_s}$) and ϵ is chosen to give the steady shock jump relation, Eq. (15). During the unsteady iteration, the value of ϵ is fixed, and the exponent α is adjusted to satisfy the unsteady shock jump condition, Eq. (16), at the upper airfoil surface. The same value of α is used at all points of the flowfield during the next time step. The conservation form of the LTRAN2 algorithm is left unchanged.

Results

In Fig. 1 the unsteady pressures for a NACA 64A410 airfoil at $M_\infty = 0.72$ oscillating in the angle of attack according to $\alpha = 2\text{ deg} + 2\text{ deg}\sin(\omega t)$, $k = 0.2$, are shown at the extremes of oscillation. In these results $q = 1.69$ in Eq. (1). It can be seen that the present method predicts a shock position about 6% chord further forward than the Euler solution.[3] This discrepancy is constant throughout the motion. However, the amplitude and phase of the unsteady shock motion are in good agreement. It is likely that the constant discrepancy can be attributed to differences in the mesh and in the numerical algorithm for the two calculations. In particular, the mesh size affects the shock capturing properties of the algorithm. In this calculation the parameter α is computed to be -0.385 and the constant ϵ is 0.083. It should be noted that a converged solution could not be obtained for this case with the standard TSD equation.

Conclusions

A procedure to correct the transonic small disturbance equation to treat strong shock waves in unsteady flow has been developed. A simplified form of this procedure has been implemented computationally. The comparisons of results of the present method with solutions of the Euler equations are adequate as regards the shock location, and good as regards the unsteady shock motion, although the pressure distribution near the leading edge is not satisfactory. The discrepancy may be due to differences in the respective meshes and in the numerical schemes. This tends to confirm the hypothesis that the error in shock location is due to the error in shock strength. Finally, although the present method gives a considerable improvement over the conventional TSD theory, it is desirable to test the present modification further in order to evaluate the technique fully.

References

[1] Murman, E. and Krupp, J. A., "Computation of Transonic Flows Past Lifting Airfoils and Slender Bodies," *AIAA Journal,* Vol. 10, July 1972, pp. 880-886.

[2] Jameson, A., "Transonic Potential Flow Calculations Using Conservation Form," *Proceedings of the AIAA 2nd Computational Fluid Dynamics Conference,* 1975, pp. 148-161.

[3] Magnus, R. and Yoshihara, H., "Calculations of Transonic Flow Over an Oscillating Airfoil," *AIAA Journal,* Vol. 13, Dec. 1975, pp. 1622-1628.

[4] Nixon, D., "Transonic Small Disturbance Theory with Strong Shock Waves," *AIAA Journal,* Vol. 18, June 1980, pp. 717-718.

[5] Klopfer, G. H. and Nixon, D., "Non-Isentropic Potential Formulation for Transonic Flows," AIAA Paper 83-0375, Reno, Nev., Jan. 1983.

[6] Ballhaus, W. F. and Goorjian, P. M., "Implicit Finite Difference Computations of Unsteady Transonic Flows about Airfoils Including the Effects of Irregular Shock Motions," *AIAA Journal,* Vol. 15, Dec. 1977, pp. 1728-1735.

[7] Liepmann, H. and Roshko, A., *Elements of Gas Dynamics,* Wiley, New York, 1957.

[8] Kerlick, G. D., Nixon, D., and Ballhaus, W. F., "Unsteady Transonic Small Disturbance Theory with Strong Shock Waves," AIAA Paper 82-0159, Orlando, Fla., Jan. 1982.

Effects of Artificial Excitation upon a Low Reynolds Number Mach 2.5 Jet

G. L. Morrison*
Texas A&M University, College Station, Texas

Introduction

THE existence of coherent structures in axisymmetric jets has been under investigation for many years. Mollo-Christensen[1] first observed coherent structures in jets by the use of space-time cross correlations in the near acoustic field. Many others have pursued the subject in a similar manner by using two probes (hot-wires, microphones, etc.) and space-time cross correlations to help identify the nature of the

Presented as Paper 81-2010 at the AIAA 7th Aeroacoustics Conference, Palo Alto, Calif., Oct. 5-7, 1981; submitted Oct. 16, 1981; revision received Sept. 24, 1982.

*Associate Professor of Mechanical Engineering. Member AIAA.